

# Nonlinear propagation of subpicosecond ultraviolet laser pulses in air

S. Tzortzakis, B. Lamouroux, A. Chiron, M. Franco, B. Prade, and A. Mysyrowicz

*Laboratoire d'Optique Appliquée, Centre Nationale de la Recherche Scientifique Unité Mixte de Recherche 7639, École Nationale Supérieure des Techniques Avancées–Ecole Polytechnique, Chemin de la Hunière, 91761 Palaiseau Cedex, France*

S. D. Moustazis

*Foundation for Research and Technology Hellas, Institute of Electronic Structure and Laser, P.O. Box 1527, Heraklion 711 10, Greece*

Received May 8, 2000

We report filamentation of subpicosecond UV laser pulses with only millijoule energy in atmosphere. The results are in good agreement with a numerical simulation using a quasi-three-dimensional propagation code.

© 2000 Optical Society of America

OCIS codes: 190.5530, 350.5400.

Intense ultrashort IR pulses launched in air undergo important changes in their propagation pattern. If the peak pulse power exceeds a critical value of  $P_{cr} \sim 10^{11}$  W, narrow filaments with radii of  $\sim 100 \mu\text{m}$  and peak intensities reaching  $\sim 10^{13}$  to  $10^{14}$  W/cm<sup>2</sup> are formed. These filaments remain stable over tens of meters or more, much longer than the beam's Rayleigh distance.<sup>1–3</sup> This self-guiding effect has been attributed to a dynamic balance between beam self-focusing (owing to the optical Kerr effect) and beam defocusing (owing to multiphoton ionization of air molecules). A signature of filamentation is the formation of a thin plasma column in the track of the self-guided pulse, owing to multiphoton ionization of air molecules. The presence of such a weakly ionized column was recently detected by electric-conductivity measurements of air.<sup>4–6</sup>

In this Letter we report nonlinear propagation of intense ultrashort UV pulses in air and their evolution into filaments. With the exception of an oral presentation at a conference,<sup>7</sup> to our knowledge filamentation with ultrashort UV pulses has not been reported, and no details on properties of such self-guided pulses are available. We have characterized the properties of these filaments by recording the beam profile and the pulse-power spectrum as a function of propagation distance. We have also verified that an ensuing plasma column is formed in the track of the self-guided pulse over a distance of several meters. These experimental results were compared with a three-dimensional numerical simulation with realistic parameters.

We obtained a UV laser pulse by doubling the output of a femtosecond dye laser and amplifying it with an excimer laser amplifier. The laser's peak emission wavelength was at 248 nm. The laser beam had a rectangular profile of 8 mm  $\times$  26 mm and a full divergence angle of  $\sim 0.15$  mrad. Its energy distribution was flat along the longer dimension of the rectangular area and Gaussian along the shorter dimension. The laser-pulse duration (FWHM) before propagation was measured by autocorrelation with NO molecules in a cell as a nonlinear medium.<sup>8</sup> The

laser could operate either in the femtosecond mode (pulse duration, 450 fs; pulse energy,  $< 10$  mJ) or in the picosecond mode (5-ps pulse duration; energy per pulse of up to 15 mJ). Measurements were obtained with 450-fs-long pulses. The laser beam was directed through a circular diaphragm of radius 3.5 mm and then focused with a lens of focal distance  $f = 9.5$  m. It was first verified that attenuated, low-intensity pulses propagated according to the laws of geometric optics.

At high intensities, strong modification of the beam propagation was observed. For incident pulse energy of  $\sim 2$  mJ and pulse duration of 450 fs, the focal spot was displaced by 2.5 m toward the lens. Half of the beam energy was lost in this new focal region. Approximately 10% of the initial beam energy propagated beyond the focus in the form of a central filament, and 40% was contained in a diverging conical beam surrounding the filament. The filament extended over a distance of approximately 4 m, with a nearly constant radius of 150  $\mu\text{m}$  (see Fig. 1, top).

The pulse-power spectrum was measured at different distances  $z$  along the propagation axis, by extraction of a weak part of the beam with an adjustable pinhole and recording of the spectrum in the far field. In the region before the focus, a small broadening can be observed. This spectral broadening becomes more pronounced once the filament is formed. The conical beam also shows spectral broadening, albeit less pronounced.

Filamentation with concomitant plasma-channel formation was verified by measurement of the electric conductance of air as a function of propagation distance by use of the conductivity technique described in Ref. 6. We measured air resistivity behind the femtosecond laser pulse by recording the current flowing between two plane metal electrodes with 4-mm holes bored in their centers to allow passage of the filament. A typical voltage of 2 kV was applied between the electrodes, which were separated by 1.5 cm. As shown in Fig. 1 (bottom), a connected plasma column extending over 6 m could be readily observed by use of this method. A rough estimate

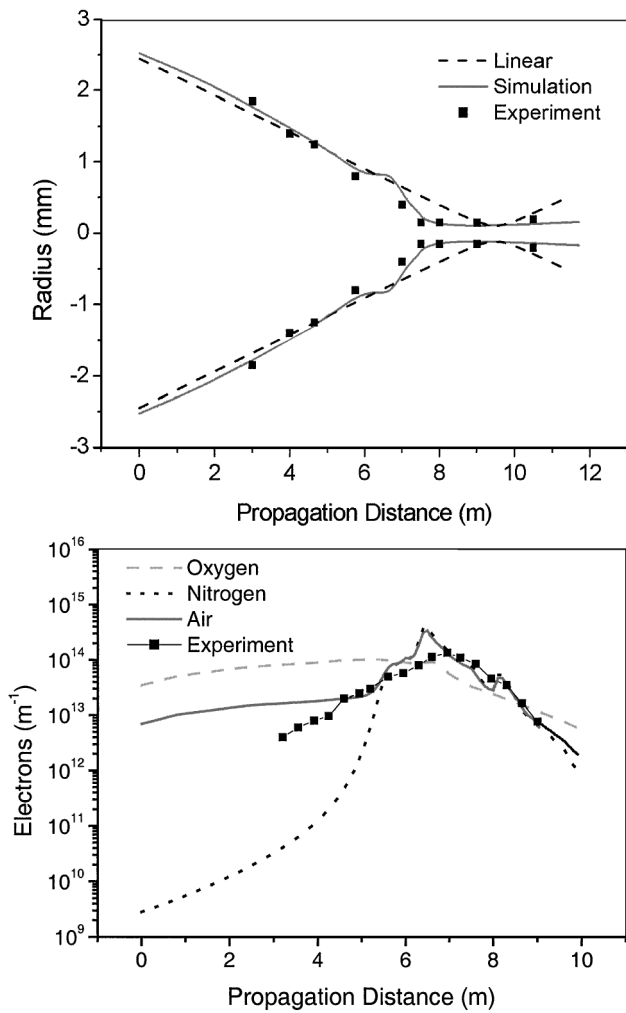


Fig. 1. Top, spatial profile of the laser beam with distance. The dashed curves correspond to beam propagation in the linear regime. Bottom, electrons per unit length measured along the propagation path, together with the numerical simulation including ionization of oxygen, nitrogen, and a gas mixture of 80%  $N_2$  and 20%  $O_2$ .

of the filament diameter was obtained from the size of a spot burned on exposed photographic film. From the measured peak current and the filament radius of  $150 \mu\text{m}$ , we extract a mean free-electron density of  $10^{16} \text{ cm}^{-3}$  in the region from 6.5 to 8.5 m (see Fig. 1, bottom).

These experimental results were compared with numerical simulations by use of a three-dimensional propagation code with axial symmetry. This code has been successfully applied to the propagation of IR femtosecond laser pulses.<sup>9</sup> The code treats nonlinear beam self-focusing that is due to the optical Kerr effect, beam defocusing that is due to multiphoton ionization of molecules with associated radiation losses, and normal beam diffraction. We adopted as the initial condition a super-Gaussian transverse beam profile to take into account the effect of the diaphragm. Beam convergence was simulated with a quadratic spatial phase factor. The initial time pulse profile was assumed to be of the form of a  $\text{sech}^2$  pulse with  $t_0 = 450 \text{ fs}$ . The initial power spectrum was

taken as a Gaussian, approximating the measured spectrum, with a flat spectral phase. Calculations were performed with different initial pulse energies corresponding to the experimental values. The value of the instantaneous nonlinear Kerr index,  $n_2 = 8 \times 10^{-19} \text{ cm}^2/\text{W}$ , was obtained from Ref. 7. We did not include the retarded Kerr effect because the laser spectrum did not exhibit a significant spectral shift to lower energies in the ionization-free region before the focus. The absence of a redshift in the first spectral moment indicates that the noninstantaneous Kerr response is small and can be neglected.<sup>10</sup> The formation of the plasma was modeled by single ionization of oxygen and nitrogen molecules, with corresponding ionization potentials of 12 and 15.5 eV, involving simultaneous absorption of three and four UV photons, respectively. Calculated free electrons produced per unit length for pure nitrogen and oxygen and for an 80%  $N_2$ -20%  $O_2$  gas mixture are shown in the bottom part of Fig. 1.

The simulation reproduces a large part of the experimental results surprisingly well. The calculated beam waist is plotted in Fig. 1 (top), together with the recorded beam diameters. Spatial repartition of the fluence at different locations, before and after filament initiation, is shown in Fig. 2. In the initial Kerr region, in which ionization does not significantly alter the propagation ( $z < 7000 \text{ mm}$ ), one can observe the formation of rings merging inward to the beam center. The appearance of ring patterns can be seen in the burning spots of the laser beam on UV photographic paper recorded at the same distance (see the insets of Fig. 2). Once a filament is formed, the trend is reversed, and light energy is radiated in the form of outward-traveling rings, in agreement with the observed conical emission. The code predicts  $\sim 8\%$  of the total initial pulse energy channeled into the filamentary core.

A striking feature emerging from the simulations is the occurrence of stable situations in which the pulse in the filamentary core stays unchanged over more than 4 m for an input energy of 2 mJ. This stability is in contrast with the results for IR filaments, which in our simulations show pulse shortening and breaking.<sup>9</sup> In this stable region the peak intensity is  $\sim 10^{11} \text{ W/cm}^2$ , 3 orders of magnitude less than in IR filaments. Yet  $\sim 25$  times more free electrons are produced; note, however, that the corresponding free-electron density is smaller by a factor of 10, since it is distributed over a larger column.

Simulations of filamentation with IR or UV pulses reveal other basic differences between the two types of filament. For UV filaments, propagation losses that are due to multiphoton ionization are significantly higher, because the number of photons involved in one ionization step is reduced from 8–10 to 3–4. Consequently, the formation of a plasma column is more pronounced than with IR pulses. For instance, we find a tenfold increase in the measured length of a connected conducting column, compared with the case of IR pulses, for similar pulse energy.

It may be worth commenting on the large differences between UV and IR filamentation. In filamentation,

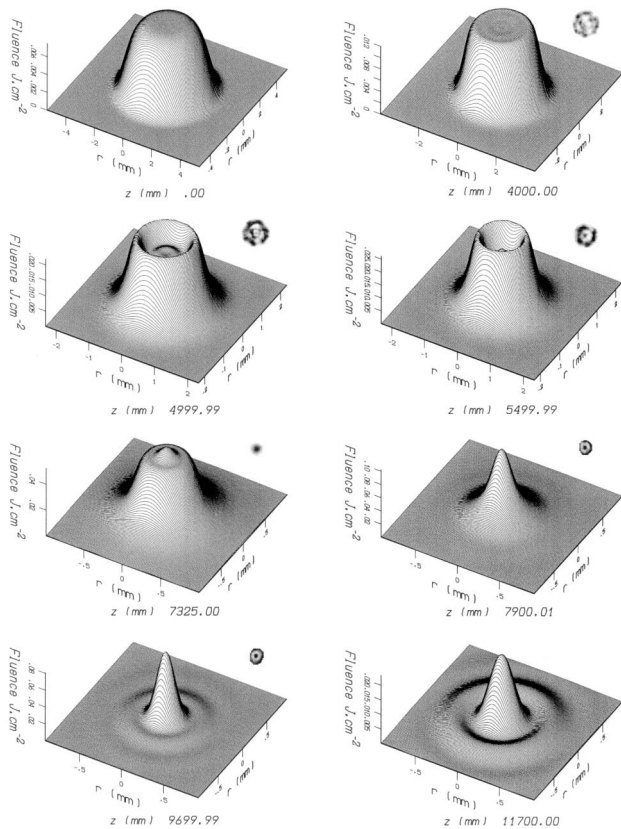


Fig. 2. Three-dimensional fluence simulated profiles for different distances. Insets, experimental burning spots of the laser on photographic paper at the same distances. The sizes of the burning spots are not to scale.

the optical Kerr effect and multiphoton absorption play crucial antagonistic roles, the first by acting as an intensity amplifier by means of beam self-focusing and the second by acting as an intensity limiter. If it is allowed to proceed sufficiently, beam self-focusing is accompanied by pulse shortening<sup>11,12</sup> and eventually pulse breakup.<sup>13</sup> Therefore the complexity of the situation depends sensitively on the value of the multiphoton cross section. With UV pulses, in which the ionization cross section is much higher, since it requires 3–4 photons instead of 8–10, beam self-focusing is hindered much earlier. The resulting situation is much simpler and closer to a true dynamic equilibrium.

We acknowledge the assistance of A. Egklezis, D. Anglos, G. Zacharakis, and C. Fotakis. This study was made possible through access to the Foundation for Research and Technology Hellas Institute provided by the European Training and Mobility of Researchers program “Access to Large Facilities.” A. Mysyrowicz’s e-mail address is mysy@ensta.ensta.fr.

## References

1. A. Braun, G. Korn, X. Liu, D. Du, J. Squier, and G. Mourou, *Opt. Lett.* **20**, 73 (1995).
2. E. T. J. Nibbering, P. F. Curley, G. Grillon, B. S. Prade, M. A. Franco, F. Salin, and A. Mysyrowicz, *Opt. Lett.* **21**, 62 (1996).
3. A. Brodeur, C. Y. Chien, F. A. Ilkov, S. L. Chin, O. G. Kosareva, and V. P. Kandidov, *Opt. Lett.* **22**, 304 (1997).
4. H. Schillinger and R. Sauerbrey, *Appl. Phys. B* **68**, 753 (1999).
5. B. La Fontaine, F. Vidal, Z. Jiang, C. Y. Chien, D. Comtois, A. Desparois, T. W. Johnston, J.-C. Kieffer, H. Pépin, and H. P. Mercure, *Phys. Plasmas* **6**, 1615 (1999).
6. S. Tzortzakis, M. A. Franco, Y.-B. André, A. Chiron, B. Lamouroux, B. S. Prade, and A. Mysyrowicz, *Phys. Rev. E* **60**, R3505 (1999).
7. X. M. Zhao, P. Rambo, and J.-C. Diels, in *Quantum Electronics and Laser Science Conference*, Vol. 16 of 1995 OSA Technical Digest Series (Optical Society of America, Washington, D.C., 1995), p. 178.
8. S. Szatmari and F. P. Schäfer, *Opt. Commun.* **68**, 196 (1988).
9. A. Chiron, B. Lamouroux, R. Lange, J.-F. Ripoche, M. Franco, B. Prade, G. Bonnaud, G. Riazuelo, and A. Mysyrowicz, *Eur. Phys. J. D* **6**, 383 (1999).
10. J.-F. Ripoche, G. Grillon, B. Prade, M. Franco, E. T. J. Nibbering, R. Lange, and A. Mysyrowicz, *Opt. Commun.* **135**, 310 (1997).
11. R. Lange, J.-F. Ripoche, A. Chiron, B. Lamouroux, M. Franco, B. Prade, E. T. J. Nibbering, and A. Mysyrowicz, in *Proceedings of the XI International Conference on Ultrafast Phenomena, 1998* (Springer-Verlag, Berlin, 1998), p. 115.
12. I. G. Koprinkov, A. Suda, P. Wang, and K. Midorikawa, *Phys. Rev. Lett.* **84**, 3847 (2000).
13. J. K. Ranka, R. W. Schirmer, and A. L. Gaeta, *Phys. Rev. Lett.* **77**, 3783 (1996).